Polymer 181 (2019) 121802

Contents lists available at ScienceDirect

Polymer

journal homepage: www.elsevier.com/locate/polymer

Design and fabrication of a low-cost pilot-scale melt-processing system

David M. Wirth, Jonathan K. Pokorski*

Department of NanoEngineering, University of California, Jacobs School of Engineering, La Jolla, CA, 92093, United States

HIGHLIGHTS

- Schematics for facile assembly of a lab scale mini-injection molding system.
- Less than $500 in raw materials, melt processes polymers at up to 250 °C with 100 MPa pressure.
- Ideal for small samples 50–500 mg total mass with low dead volume.
- Non-newtonian modeling of shear rate inside melt processing system.

ARTICLE INFO

Keywords:
Melt processing
Composites
Injection molding
Polymer engineering

ABSTRACT

Melt processing of polymeric materials is a ubiquitous technique for forming, shaping, refining and homogenizing polymers and polymer composites. Melt-processing techniques are the primary manufacturing method of consumer and industrial thermoplastic parts, especially when using commodity polymers with high-throughput production. Melt-processing, however, is underutilized in academic laboratories when developing high value-added materials due to the capital expense of the equipment and relatively large-scale required to carry out such processing. These concerns make pilot-scale melt-processing challenging, particularly for the development of new polymers or polymer composites where materials can only be generated in small-scale at reasonable costs. The current study designs and evaluates a bench-top, sub-milliliter volume extrusion and injection-molding device, which sources parts from current 3D printer technology at minimal expense. The plans presented will open this convenient technique to academic research laboratories interested in pilot-scale experiments. A systematic approach to melt processing of PLA, PLGA, and PCL polymer composites is demonstrated. Characterization of the dispersion of pharmaceuticals, small molecules and nanoparticles in melt processed polymers is presented as a demonstration of potential utility.

1. Introduction

Melt processing is the most versatile manufacturing technique used in the plastics industry to produce objects with different size, shape and function [1–3]. Melt processing most notably includes techniques such as extrusion, injection molding (IM), and blow molding. The power of melt processing in industrial manufacturing is immense as these processes are continuous, solvent free, and massively scalable [4]. Melt-processing has commonly been used for cosmetic/pharmaceutical packaging and, more recently, for the production of biomedical devices such as tissue engineering scaffolds, microneedles, microfluidic devices, and for the preparation of controlled release drug delivery systems [5–11]. The versatility of melt-processing techniques can be exploited for the production of drug delivery systems with defined shape and or/dimensional characteristics that control their release parameters within the body [12–15]. Melt-processing offers great advantages in the pharmaceutical arena due to its high potential for scalability and repeatability. Furthermore, the process avoids the use of solvents, which is helpful in terms of manufacturing speed, shelf-life, reproducibility and safety of the products produced by this method [15]. The use of both pressure and heat during melt-processing also serves to sterilize the molded components, reducing microbial contamination, increasing the dissolution rate and possibly improving the bioavailability of poorly soluble drugs administered by this method [16–18]. One particular challenge to the melt-processing of drug delivery devices is the strict control of the homogeneity of such devices, i.e. ensuring the substance to be released over time is well-distributed throughout the device and not aggregated [19]. Another challenge is the elimination of voids which could cause inhomogeneities in devices made from high value materials.

* Corresponding author. 9500 Gilman Dr., SME Building 243J, La Jolla, CA, 92093, United States.
E-mail address: jpokorski@ucsd.edu (J.K. Pokorski).

https://doi.org/10.1016/j.polymer.2019.121802
Received 19 July 2019; Received in revised form 10 September 2019; Accepted 11 September 2019
Available online 12 September 2019
0032-3861/

Injection molding is one form of melt processing whereby a molten polymer is forced into a mold using high pressure and temperature [1]. Traditional IM is accomplished by feeding polymer pellets or powder contained in a hopper through a heated nozzle and barrel by means of a mechanical augur or metering screw [1]. A mold is placed at the output of the heated nozzle and held against the nozzle by means of a hydraulic, pneumatic or other type of mechanical actuator. As the mold fills with molten polymer, it may be maintained at a desired temperature with cooling channels. After the molten polymer has filled the mold, the product is cooled rapidly and solidifies in the desired shape, which is then ejected at the end of a single injection cycle. This cycle can be repeated indefinitely to produce large volumes of identical polymer parts and forms the basis for many economies of scale in today's manufacturing industry. IM is a mature technique, which was first developed near the end of the 1800's, and experienced a great deal of interest around the 1940's with the invention of the first polymetric materials such as bakelite [20]. Since then, further improvements have been made to the process in the form of advanced automated industrial machines, co-rotating and counter-rotating screw extruders, advanced molds with integrated cooling channels for faster throughput, and multi-material injection molding [21,22]. Recently, microinjection molding has gained favor whereby parts can be manufactured in volumes as low as 1 cm^3, and some specialty systems are designed for volumes as low as 0.082 cm^3 [24]. However, the cost of such instrumentation is exceptionally high, precluding the use of these techniques for pilot-scale academic research. Therefore, it would be extremely beneficial to the academic research community to perform IM at pilot-scale prior to a significant capital investment to scale up to commercial equipment.

Recently, studies have been carried out on lab-scale mini-injection molding of drug-delivery capsules, but the equipment needed for such studies remains large and expensive relative to the budget of most academic research labs, leading many in the field to forego the use of IM in favor of more economical alternatives [23]. In addition, due to the large scale and consequently large dead-volume of such traditional techniques, high value research materials may be impractical to process in such a manner. Even the smallest commercially available injection molding machine would require tens to hundreds of grams of material – an impractical amount for many academic labs which produce samples on the milligram to gram scale.

Our laboratory seeks to use melt-processing to manufacture protein-polymer composites, of which novel protein components are a precious and expensive resource [19,24,25]. Hence, we sought to develop a simple instrument that could be made accessible to the research community, which yielded reproducible melt-processing results. The work described herein aims to address issues of cost and scale in polymer-processing in order to open melt-based processing to a wider community. Described in this manuscript are the design and fabrication of a plunger-based melt processing system for extrusion and injection molding. The system does not fully recapitulate a screw-based processing system since it has no mixing capability, nevertheless we have found that the machine fills a capability gap and its mixing capabilities are adequate for most screening applications. This bench-top system can process polymer and composite materials at scales below 0.02 cm^3 and can be fabricated at 2–3 orders of magnitude lower expense than commercially available microinjection molders (Fig. 1). Furthermore, a range of polymer composite materials are described along with a variety of self-made molds fabricated by CNC to dictate part geometry.

2. Materials and methods

2.1. Materials

Polycaprolactone (PCL) powder (Cellink Part #TP60505001, MW 50 kDa), Poly lactic-co-glycolic acid (PLGA) powder (Polyscitech, AP041, MW 5–25 kDa) were extruded as received. Polylactic acid (PLA) filament was purchased from Amazon (B07D699XT5), and high purity PLA was also obtained from Cellink (lot no. 7766). Tetrahydrofuran (THF) was purchased from Fisher (ACS reagent). Each polymer composite was fabricated with varying amounts of nickel-coated multi-wall carbon nanotubes (MWCNT) (US Research nanomaterials, Inc., part number US4430), ferrocene (Sigma), and doxorubicin (TSZ Chemicals, RYG02), which were added according to Table 1. Parts for melt-processing equipment fabrication are detailed in the supplementary information.

2.2. Methods

2.2.1. Benchtop injection molding instrument fabrication

The design of the desktop melt-processing system began by leveraging existing 3D printer technology and commercially available 3D printer parts (Fig. 2). The core of the system is an ordinary Fused Deposition Modeling (FDM) 3D Printer heater block. This extruder was mounted on a 1.5″ T-slotted aluminum rail with removable gusset which facilitates easy removal of the extruder for loading of polymer material and cleaning. A pneumatic cylinder and 3D printed shaft collar were also mounted onto the rail and secured into place with gussets. Two shaft collars were 3D printed and designed to secure both 5/64 x 3” and a 3 x 75 mm stainless steel rods into position with thumb screws which allow for ease of removal of the rods for cleaning. We focused on a piston-based approach rather than a more conventional augur design due to its simplicity, cost effective construction and effectiveness at minimizing dead volume to allow for smaller batch sizes. If mixing is deemed inadequate for particular applications, the system is modular and a static mixing element could be incorporated downstream of the plunger.

Lab air at 690 kPa was routed through an adjustable air regulator and 5-way valve to the two ports on the cylinder which allow for the piston to be extended and retracted at the touch of a button and the pressure to be independently adjusted by means of the regulator during extrusion. The ceramic cartridge heater and thermocouple were connected to a commercial PID controller, which was powered by a 300 W 12 V power supply. The output of the PID controller was connected to the gate of an enhancement mode MOSFET which was used to switch the ground wire of the heater cartridge. Finally, electrical components were housed in a 3D printed PLA enclosure. The electrical and pneumatic connections are illustrated in Fig. 2. Assembly instructions, pneumatic and electrical schematics, STL files and CAD diagrams can be found in supplemental information. It is important to note that the PID controller must be manually tuned to reduce overshoot – we found the following values worked well on the Inkbird ITC-106VL thermal controller: P = 3, I = 1, D = 450–3000. In tuning the PID, we aimed to minimize overshoot, but the actual heater block temperature setting of the controller should be set according to the polymer being extruded. It is important to set the block temperature to a value between the melting point and decomposition point of the polymer being processed (i.e. between 160 and 300 °C for PLA).

2.2.2. Injection mold fabrication

Aluminum injection molds (Fig. 3) were CNC machined on a Tormach PCNC1100. These molds consist of two halves, each 0.25” thick which are held together by M3 screws. The static mold half consists of a male M6 threaded port which screws into the extruder heater block. A M6 threaded barrel is loaded with a removable PTFE sleeve and sample of polymer to be extruded, then screwed into the heater block from the opposite end, creating a seal with the static mold half. The patterned mold is then screwed onto the threaded holes in the static mold. The heater block is brought to operating temperature (between 60 and 250 °C) and the pneumatic piston is activated to inject the molten polymer into the mold. After injection, the mold may be left to cool, unscrewed and separated to remove the polymer samples.

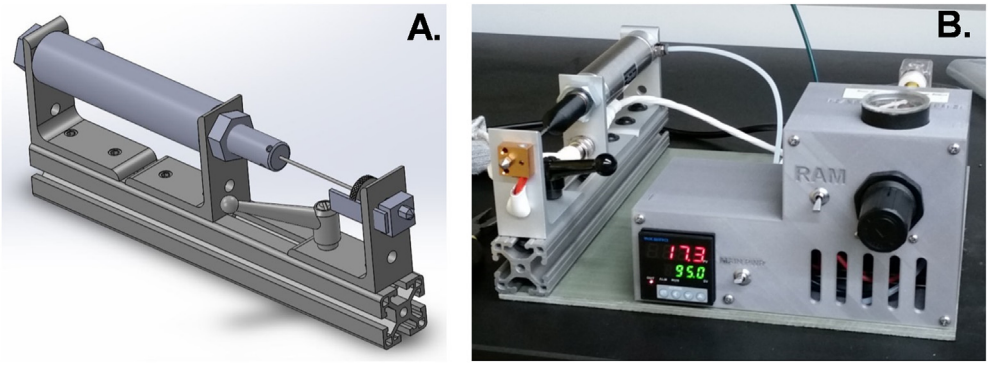

Fig. 1. A) Mechanical design of pneumatic injection system, B) digital image of micro-injection molding instrument.

Table 1
Composition of samples 1-8 prepared for injection molding.

#	Polymer	Polymer mass (mg)	Filler	Filler mass (mg)	Extrusion Temp. (°C)	Extrusion Pressure (MPa)	Injection Temp. (°C)	Injection Pressure (MPa)
1	PLA	500	None	N/A	210	10	210	50
2	PLA	500	Ni-coated MWCNT	50	210	10	210	50
3	PLA	500	Doxorubicin	1	190	10	190	70
4	PLGA	250	Doxorubicin	5	90	10	90	10
5	PCL	500	Doxorubicin	10	80	6	80	35
6	PCL	500	Ni-coated MWCNT	50	80	6	80	35
7	PCL	500	Ferrocene	10	80	6	80	35
8	PCL	500	None	N/A	80	6	80	35

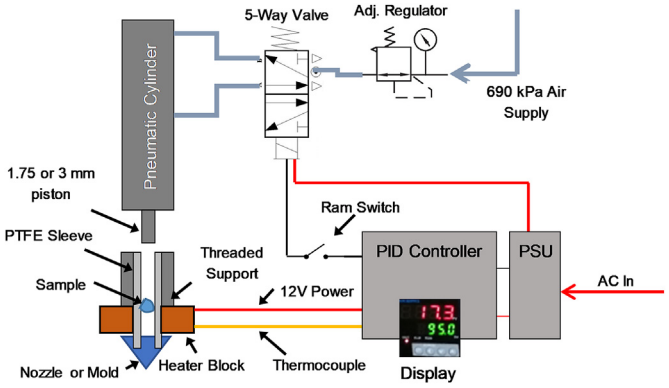

Fig. 2. Design schematic of bench-top polymer melt processing system.

2.2.3. Polymer composite fabrication

The following polymer samples (Table 1) were prepared for co-extrusion with PLA, PLGA, and PCL powders. PLA samples were prepared by dissolving PLA filament in 30 mL of THF and then sonicating with the filler species at 30 W power for a pulse period of 5 s on and 10 s off for a total time of 5 min, then rotary evaporated at 25 °C/120 rpm and vacuum desiccated for 24 h over sodium hydroxide. PLGA and PCL samples were prepared in Eppendorf tubes and the raw powders mixed via vibratory shaking for 60 s before loading the mixed powders directly into the extruder.

The dried PLA films and the PCL and PLGA powdered samples were then placed into 3 mm PTFE sleeves and individually inserted into the extruder following the procedure below.

For each sample: the extruder was brought up to temperature and left to stabilize for 5 min after reaching its set point, then the regulator was brought up to its desired pressure, and the polymers were pre-extruded through a 0.8 mm stainless steel nozzle in the case of PLA, and a 0.6 mm nozzle in the case of PLGA and PCL as shown in Fig. 4A. This first extrusion step was carried out in order to homogenize the polymer with the dispersed phase. The extrudate cylinders were then re-loaded into a fresh PTFE sleeve and inserted into the barrel, then an injection mold was screwed into the opposing side of the heat block in place of the nozzle. A thin layer of silicone oil (1 wt%) in xylene or a commercial mold release such as CRC 03300 may be applied to the mold halves prior to assembly in order to aid in extraction. The extruder was then brought up to temperature and left to stabilize its temperature for 5 min after reaching its set point, the regulator pressure was brought to its set point, and the polymers were injected into molds. The mold section was then unscrewed from the heater block while hot using a pliers or heat resistant glove and the mold cooled by placing briefly on a bed of crushed ice. Once cooled, the mold was unscrewed and the sample extracted. After each extrusion, the PTFE sleeve was also replaced, and all parts were cleaned with appropriate solvents. SEM and EDS were carried out using a FEI Quanta 600 SEM and Bruker XFlash 6/60 Energy Dispersive X-Ray Spectroscopy.

3. Results and discussion

3.1. Injection molding of polymer composites

We aimed to investigate three different polymers and their composites: PLA, PCL, and PLGA due to their biocompatibility, low melting temperature and low melt viscosity. Using these three polymers and three dispersed species: Ferrocene, MWCNT and Doxorubicin, we intended to demonstrate the capacity of the current system to process and shape devices from a variety of value-added materials in small batches with a uniform distribution of dispersed fillers. MWCNT coated with a thin layer of Ni were chosen due to their heavy metal content (useful for EDS characterization of dispersion) and its unique fibrous structure which is an excellent analogue for 1-dimensional polymer additives, also their tendency to aggregate simulates a worst-case scenario to highlight the conclusions of this study. Ferrocene was chosen as a lipophilic small molecule additive with a heavy metal ion (again for EDS), and doxorubicin was chosen as a small molecule additive which was representative of the types of organic therapeutics used in medical implanted devices.

Composites were first extruded into thin cylinders to compound and homogenize the materials (Fig. 4A) followed by IM into defined form

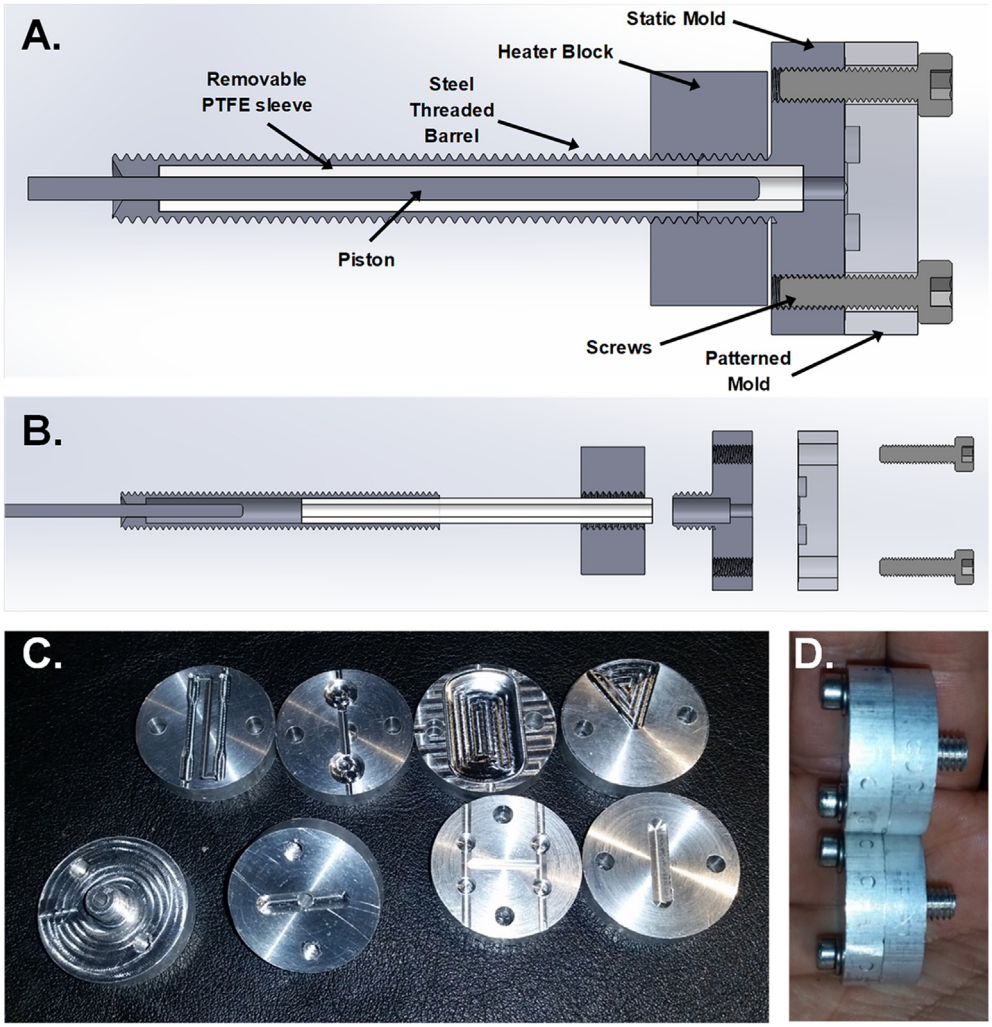

Fig. 3. Injection molding component. A) Assembled model of injection molding system. B) Expanded model of injection molding system. C-D, Aluminum injection molds used throughout the current study, C) From top-left to right: dog bones, large disks, DLP mold, ribbon extruder. From bottom-left to right: standard nozzle, cylinder nozzle, small disks, cylinder mold. D) fully assembled molds.

factors as determined by the molds. Flashing (over-extrusion of material) was observed in all parts and was not detrimental to part geometry (Fig. 4B). The flashing was very thin and was easily peeled away with a scalpel and flush cutters. Injection molded polymer samples 1–4 are shown in Fig. 4C, and samples 5–8 are shown in Fig. 5B with the flashing removed.

3.2. Characterization of composite samples

To assess the dispersion of additives in our polymer melt processed samples, Energy Dispersive X-Ray Spectroscopy (EDS) was chosen as a characterization technique due to its ability to examine the microscopic distribution of heavy atoms throughout a sample. After injection molding and cleanup, samples were sliced into thin sections using a razor blade, carbon coated, and then imaged using EDS. Samples 1–4

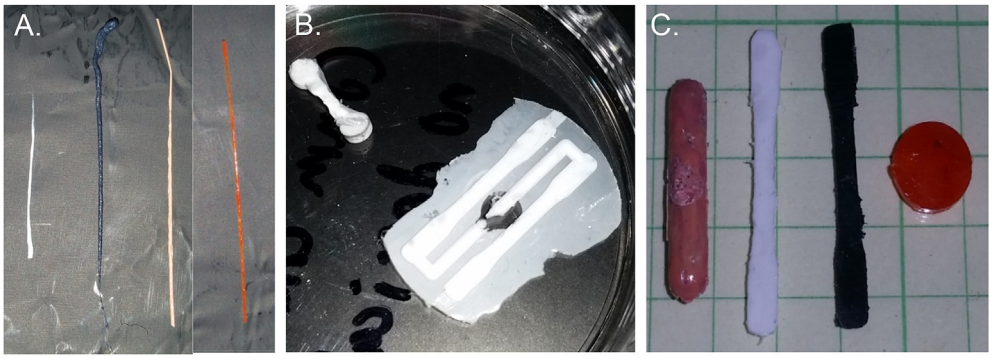

Fig. 4. Melt processing of polymer samples; A) samples 1–4 (from left to right) showing extrudate cylinders after first extrusion, B) flashing of PLA directly after injection molding of sample 1, C) de-flashed PLA and PLGA injection mold samples 3,1,2,4 (grid squares 5 × 5 mm).

Fig. 5. A) aluminum dog bone injection mold used during the current study, B) successfully injection molded PCL samples 5–8 (from left to right); Doxorubicin, MWCNT, Ferrocene, and pure PCL.

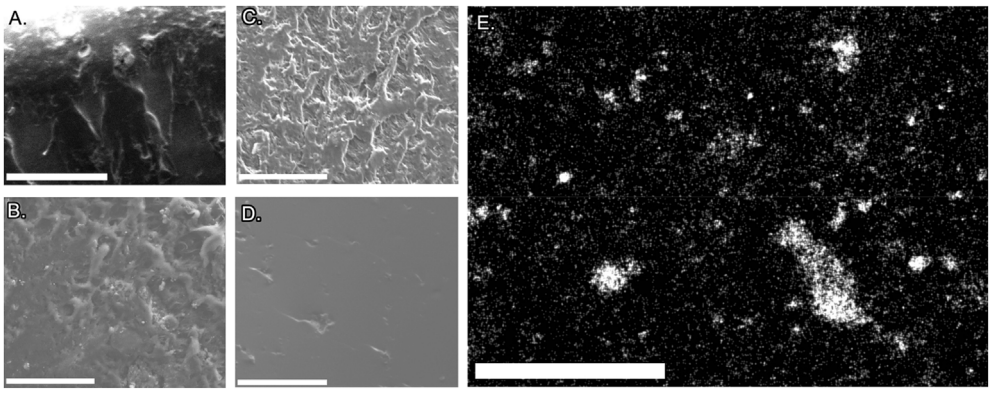

Fig. 6. Electron micrographs of PLA-based samples: A) Sample 1 - PLA only, B) Sample 2 - PLA/MWCNT, C) Sample 3 - PLA/Doxorubicin, D) Sample 4 - PLGA/Doxorubicin, E) Ni Kα EDS of sample 2. All scale bars 100 μm.

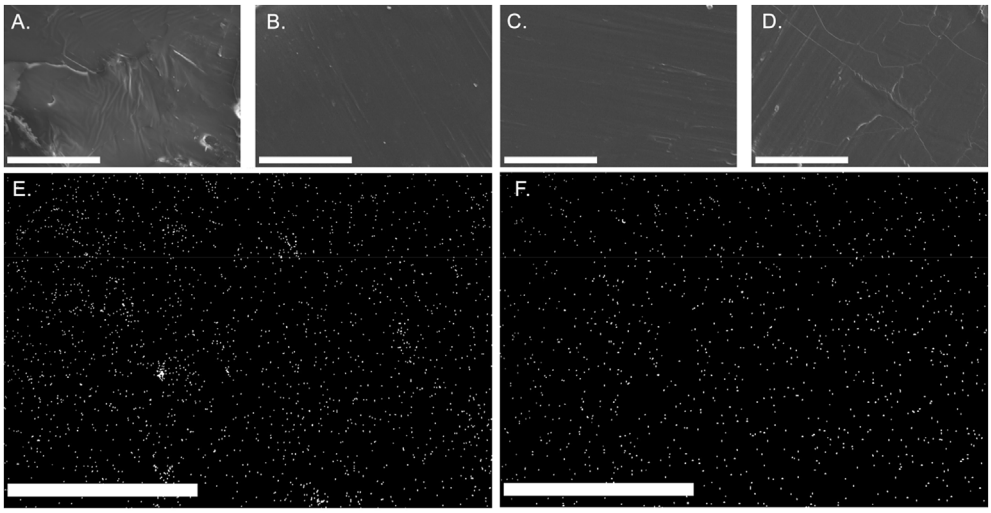

Fig. 7. Electron micrographs of PCL samples: A) Sample 5 - PCL/Doxorubicin, B) Sample 6 - PCL/MWCNT, C) Sample 7 - PCL/ferrocene, D) Sample 8 - PCL control, E) Ni Kα EDS of sample 6, F) Fe Kα EDS of sample 7. All scale bars 100 μm.

are visualized in Fig. 6 and samples 5–8 are seen in Fig. 7.

PLA samples Fig. 6A–C showed structural morphology consistent with the presence of microvoids – macroscopic voids can also be observed in the PLA samples in Fig. 4. We suspect that PLA samples exhibited higher porosity due to trapping of air in the twisted extruded films and potentially due to the presence of solvents trapped inside the polymers themselves which expand during high temperature molding and extrusion. Our PLGA sample Fig. 6D, showed similar behavior and porosity to the PCL samples and was also processed without the use of solvents. We observe few voids in the PCL samples under electron microscopy Fig. 7A–D, largely thanks to the solvent-free nature of the polymer processing. However, due to the low melting point of PCL, we had some difficulties imaging samples under high magnification electron microscopy as samples tended to heat, outgas and melt in the vacuum chamber as the electron beam scan area decreased at higher magnification.

The samples which were never exposed to solvents tended to show far lower porosity, likely because they were extruded as powders. This allowed for pre-compression of the blended materials eliminating unwanted air during the compounding process.

EDS results were taken via mapping of Ni and Fe Kα signals of samples 2, 6 and 7 with respect to position. EDS of other samples were not acquired due to the lack of heavy metal atoms in such samples. Most telling were the EDS maps of samples 2 (PLA/MWCNT) and 6 (PCL/MWCNT), Figs. 6E and 7E respectively. Fig. 8 shows a composite of both EDS Ni Kα maps overlaid on SEM images of samples 2 and 6 and shown side-by-side to elucidate the difference in additive dispersion between solvent and melt-processed samples.

Due to the nickel content of the MWCNT and the iron content of Ferrocene, aggregative behavior of filler species can easily be observed via EDS. Fig. 8 shows low aggregation in the Ni Kα EDS of Sample 6, and a fair amount of aggregation in the Ni Kα EDS of Sample 2 where the Ni-coated MWCNT tended to cluster at various locations in the PLA samples processed using solvent-based techniques. Based on these

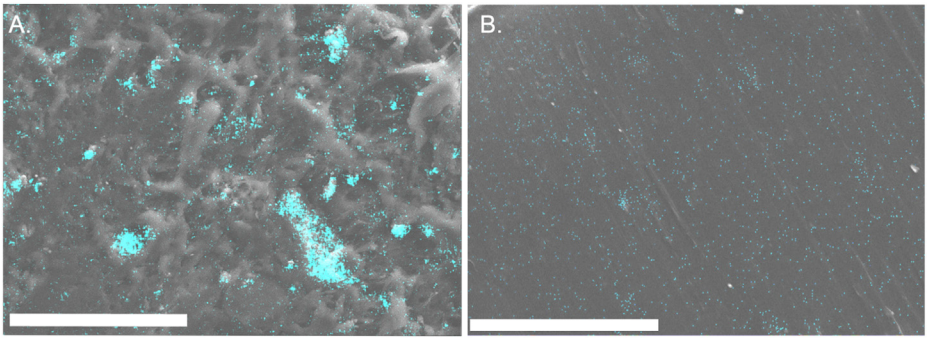

Fig. 8. EDS/SEM composite micrographs of Ni Kα EDS map overlaid on SEM images A) Sample 2: PLA/MWCNT, B) Sample 6: PCL/MWCNT. All scale bars 100 μm.

micrographs, we observe a marked decrease in aggregation of nanoparticles in the PCL samples injection molded via a solvent-free process. Structural morphology also shows far fewer defects in samples prepared via solvent free-processes.

An additional set of samples were prepared from high purity PLA powder specifically for mechanical analysis, these samples were loaded with a much lower concentration of Ni-doped MWCNT as shown below in Table 2. SEM micrographs and EDS maps of the samples are provided in supplemental figures.

Samples 9–12 were prepared in Eppendorf tubes and mixed via vibratory shaking for 60 s before loading the powders directly into the extruder. Samples 13–16 were prepared by dissolving PLA and MWCNT in 30 mL of THF and sonicated with the filler species at 30 W power for a pulse period of 5 s on and 10 s off for a total time of 5 min, then rotary evaporated at 25 °C/120 rpm and vacuum desiccated for 24 h over sodium hydroxide. All samples were pre-extruded at 210 °C/6 MPa and only the temperature and pressure in the final injection molding step was varied between samples. Four additional control samples were also prepared in an identical fashion to samples 9–12 without the use of solvent and also without the addition of Ni-coated MWCNT to determine if the addition of MWCNT affected the overall mechanical properties of the composite parts.

Samples geometry was designed based on ASTM D638 “Standard Test Method for Tensile Properties of Plastics” and ASTM D1708 “Microtensile Testing of Plastics” was also considered in the experimental design. Since even the smallest test sample in ASTM D1708 required a larger sample than the mold, we used the ASTM D638 Type I profile scaled down to the appropriate size. ASTM D638 specifies that in specimens in samples thinner than 1 mm, ASTM D882 is the “preferred” test method, but D638 is still valid.

Samples were weighed and tested on a CellScale Univert mechanical testing apparatus with 100 N load cell. As noted by ASTM D1708, the elastic modulus obtained from this testing greatly deviated from literature values, and this was to be expected. However; the tensile strength and elongation at break was reasonably similar to reported literature values [26]. Fig. 9 shows the sample geometry and summary of mechanical properties; tensile strength was largely independent of extrusion parameters (i.e. temperature and pressure) for the solvent-free samples, but strength was greatly reduced in the solvent-processed samples and was strongly correlated to processing temperature.

The weight of samples was divided by the sample volume (since injection molds were CNC machined from a CAD model of known volume) and used to compute the average density for samples processed with solvent and without solvent. The results of the density study are listed below in Table 3. It is important to note that the density, ultimate tensile strength and elongation at break for solvent-free injection molded samples was remarkably close to that of the literature values (despite the addition of 2 wt% CNT, which may account for the slightly lower elongation and higher tensile strength).

3.3. Simulation of shear forces

Since many of the applications for such a small-scale desktop injection molding system involve the preparation of sensitive biological samples, we simulated the forces exerted during extrusion, specifically shear rate. Many biomedical applications (such as the delivery of proteins and pharmaceuticals) are heat or shear-rate sensitive [28]. Specifically, Lee et al. examined the effect of shear rate on the stability of viral nanoparticles and found they were stable within a narrow window between 10 and 25 s^{-1} shear rate [24]. In order to precisely predict and control the shear rate inside our system, we developed a non-Newtonian model using a Carreau-Yasuda dynamic viscosity approximation with boundary slip to estimate the shear rate for a given chamber pressure and nozzle size in order to produce more consistent results with biological samples [29]. Because the ratio of pneumatic piston diameter to barrel bore diameter determines the nozzle pressure. This allows for the exertion of very high pressures in the barrel of the extruder, which might result in high shear rates at the nozzle. Since the area ratio is proportional to the square of the pressure ratio: 690 kPa (0.69 MPa) of air pressure driving the main 31.75 mm bore pneumatic cylinder will apply a force of up to 690 N to a small shaft which is mechanically coupled to the cylinder output, resulting in a barrel pressure which is 690 N/(shaft area in m^2) Pa. In short: this results in a 257x multiplication of the applied pressure to the polymer inside the extruder barrel for a 1.75 mm shaft, or an 87.5x multiplication for a 3 mm shaft. It should be noted that the barrel and nozzle pressure is

Table 2
Composition of samples 9-16 prepared for injection molding followed by mechanical testing.

#	Polymer	Polymer mass (mg)	Filler	Filler mass (mg)	Extrusion Temp. (°C)	Extrusion Pressure (MPa)	Injection Temp. (°C)	Injection Pressure (MPa)
9	PLA	500	Ni-coated MWCNT	10	210	6	210	30
10	PLA	500	Ni-coated MWCNT	10	210	6	210	12
11	PLA	500	Ni-coated MWCNT	10	210	6	230	12
12	PLA	500	Ni-coated MWCNT	10	210	6	250	6
13	PLA	500	Ni-coated MWCNT	10	210	6	210	30
14	PLA	500	Ni-coated MWCNT	10	210	6	210	12
15	PLA	500	Ni-coated MWCNT	10	210	6	230	12
16	PLA	500	Ni-coated MWCNT	10	210	6	250	6

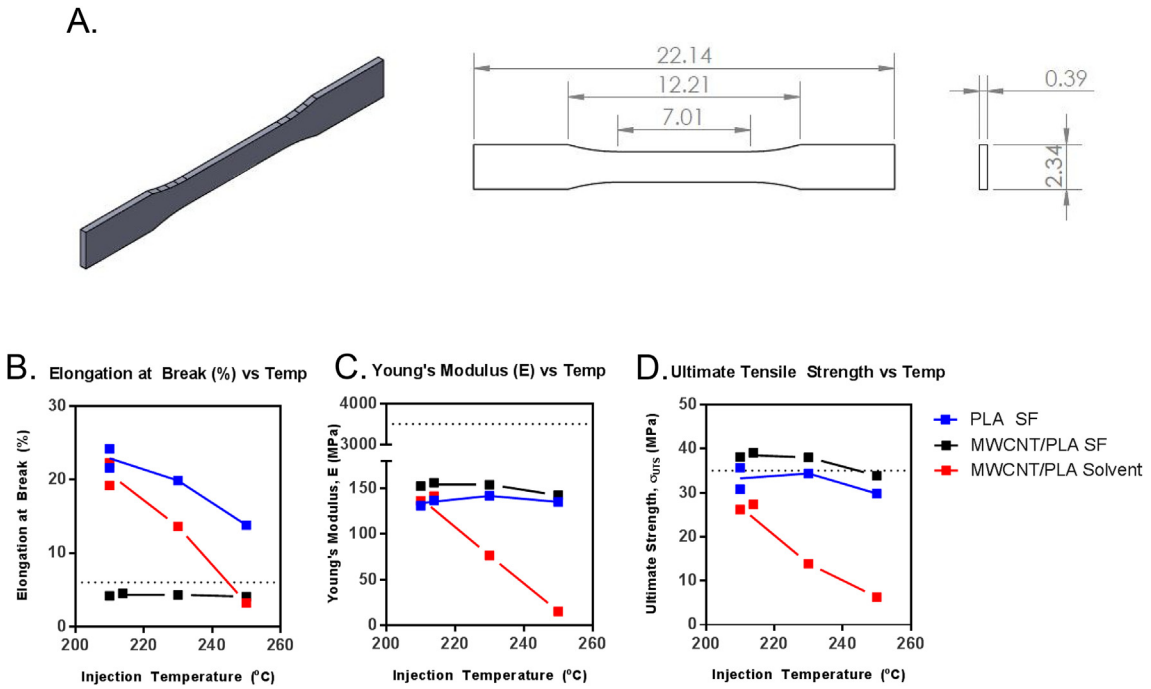

Fig. 9. Mechanical properties as a function of processing temperature and use of solvent during pre-processing. SF indicates Solvent Free processing. A) Physical dimensions of test samples (mm), B-D) mechanical properties as a function of injection molding temperature, the literature value for unfilled pristine PLA is shown as a dashed line on all graphs.

Table 3
Mean values of properties for PLA + MWCNT tensile test samples prepared with and without solvent.

PLA Properties	Literature [27]	Solvent Free	Solvent Processed
Density (g/cm^3)	1.24	1.236	1.197
Elongation at Break (%)	2–9	4.3	15.3
Ultimate Tensile Strength (MPa)	36–77.1	37.3	18.7

largely independent of any fluid properties of the polymer melt due to the largely incompressible nature of fluids (including polymers) [30] in laminar flow regimes. Warfield et al. demonstrates that the compressibility of bulk polymers is negligible (< 5% ΔV/V) at pressures below 1000 atm (100 MPa). Even in highly flow-restricted systems such as injection molding, incompressible flow can still safely be assumed due to the low flow rate, which allows the fluid pressure to equalize before compressibility effects occur [31]. Therefore: incompressible and laminar flow was assumed for the purpose of simulation and a theoretical model was created in COMSOL to predict shear rates of polymer mixtures for various nozzle and barrel diameters as shown in Fig. 10.

From this model it can be observed that the maximum shear rate is largely independent of the barrel diameter and depends primarily on the nozzle size and barrel pressure. Furthermore, it can be observed that the maximum shear rate increases with increasing nozzle size, due to the increased speed of the polymer extrusion through the larger nozzle. Therefore, for future applications of this system, it is important for users to keep in mind that extruder shear rate is directly proportional to speed of extrusion. If higher barrel pressures are required for extrusion of a particularly viscous polymer, shear rates can be kept low by simply reducing extrusion speed (by adjusting the regulator pressure) in a constant-pressure extrusion system.

4. Conclusion

A bench-top melt-processing system has been designed and developed. Such a device allows academic researchers access to melt processing technology which previously was cost and scale prohibitive. Such a system serves as a melt-processing test bed, allowing individual labs to run pilot studies on very small batches of material, accelerating development of devices made from a range of high value-added components. Its methods of fabrication and cost of acquisition ($300) put it well within the reach of research labs across a wide variety of disciplines which may not have considered the use of melt-processing due to its large capital investment in injection molding equipment. The fabrication of molds was challenging; however, due to the rise in availability of distributed manufacturing services such as 3DHubs – the cost of fabrication of custom molds for this device (roughly $200/mold, files included in supplemental information) is far lower than the cost of traditional injection mold tooling for parts of a similar size ($1000+). Furthermore, reducing the size and cost of IM to a desktop machine allows for individual research labs to tailor machine specifications and controls to individual laboratory needs (such as sterility, optimization for small quantities of material, etc.)

Samples of melt-processed polymer were characterized via SEM and EDS for distribution of composite species and presence of gas inclusions. Our efforts to eliminate gas pockets were largely successful in PCL and PLGA due to the solvent-free nature of these polymer preparations. We suspect their lack of aggregation is due to the good wettability of additives with the polymer melt during processing, allowing the molten polymer itself to act as a solvent. Uniformity may be improved by incorporating a static mixer to the barrel, by increasing the temperature to allow for lower viscosity in the polymer melt, by increasing the pressure to allow for higher shear rate and thus more vigorous mixing in the nozzle throat, or by increasing the number of pre-extrusion cycles to allow for a more complete mixing of the additive with the polymer. It is unknown at this time the effect of additive miscibility with the polymer melt on aggregation – further experiments may be conducted on highly polar additives (such as salts) with highly non-polar polymers (such as PCL) to determine the aggregative behavior in these mixed polarity systems. In PCL, the distribution of composite species was very uniform using a solvent-free approach, and little to no microscale or macro-scale aggregation was observed in samples

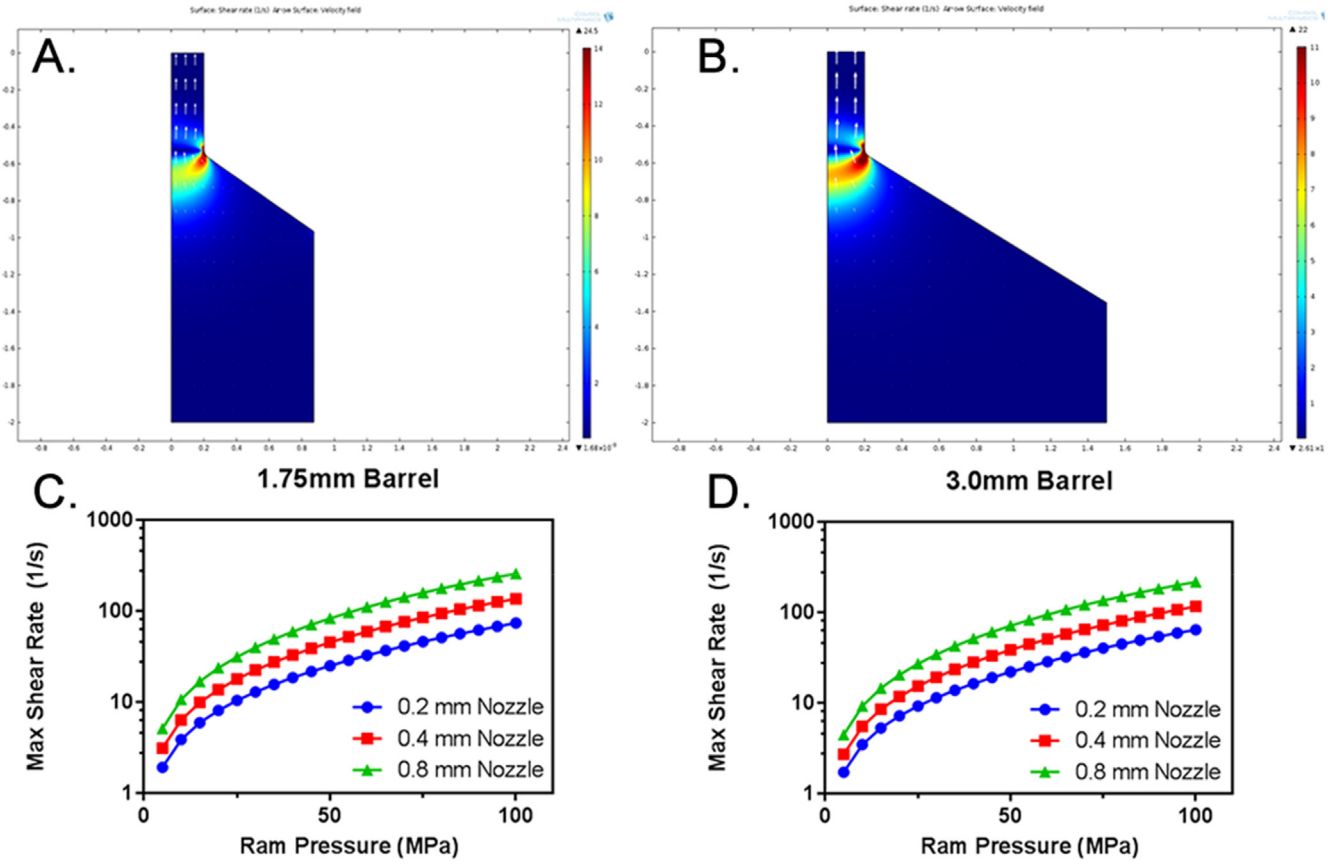

Fig. 10. Theoretical max shear rate in nozzle as a function of barrel pressure, barrel diameter, and nozzle diameter. A-B, simulation of shear rate as a function of position at 36 MPa pressure for A) 1.75 mm diameter bore, B) 3.0 mm diameter. C-D, simulations of maximum shear rate as a function of pressure and nozzle exit diameter for C) 1.75 mm bore, D) 3.0 mm bore.

processed without the use of solvents. In PLA, the distribution of composite species was largely dependent on shear rate; samples injected at higher pressure showed far lower aggregation than samples injected at lower pressure and higher temperature. Through our testing, we concluded that there was no clear correlation between mechanical strength of specimens and their injection molding properties in solvent free PLA for the temperature and pressures tested. There was, however, a statistically significant effect whereby the use of solvents in the processing of polymer samples resulted in a decrease in mechanical properties and the magnitude of this effect was proportional to the injection temperature. Overall, we believe the current method is a beneficial tool for users across a wide variety of disciplines and may serve to facilitate discoveries and solutions which otherwise may not have been feasible.

Ackowledgments

D.M.W. and J.K.P. acknowledge funding from the National Science Foundation (OISE 1844463) and UCSD.

Appendix A. Supplementary data

Supplementary data to this article can be found online at https://doi.org/10.1016/j.polymer.2019.121802.

References

[1] L. Zema, G. Loreti, A. Melocchi, A. Maroni, A. Gazzaniga, Injection molding and its application to drug delivery, J. Control. Release 159 (3) (2012) 324–331 https://doi.org/10.1016/j.jconrel.2012.01.001.
[2] D.M. Bryce, Plastic Injection Molding: Manufacturing Process Fundamentals vol. 1, Society of Manufacturing Engineers, Dearborn, 1996 vol. 1.
[3] M. Kamal, Injection Molding; Technology and Fundamentals, Hanser Publications, 2009.
[4] L. Zema, G. Loreti, A. Melocchi, A. Maroni, A. Gazzaniga, Injection molding and its application to drug delivery, J. Control. Release 159 (3) (2012) 324–331 https://doi.org/10.1016/j.jconrel.2012.01.001.
[5] H. Haugen, J. Will, W. Fuchs, E. Wintermantel, A novel processing method for injection-molded polyether–urethane scaffolds. Part 1: processing, J. Biomed. Mater. Res. B Appl. Biomater. 77B (1) (2006) 65–72 https://doi.org/10.1002/jbm.b.30396.
[6] M.E. Gomes, A.S. Ribeiro, P.B. Malafaya, R.L. Reis, A.M. Cunha, A new approach based on injection moulding to produce biodegradable starch-based polymeric scaffolds: morphology, mechanical and degradation behaviour, Biomaterials 22 (9) (2001) 883–889 https://doi.org/10.1016/S0142-9612(00)00211-8.
[7] F. Sammoura, J. Kang, Y.-M. Heo, T. Jung, L. Lin, Polymeric microneedle fabrication using a microinjection molding technique, Microsyst. Technol. 13 (5) (2007) 517–522 https://doi.org/10.1007/s00542-006-0204-1.
[8] Y. Zhang, K. Brown, K. Siebenaler, A. Determan, D. Dohmeier, K. Hansen, Development of lidocaine-coated microneedle product for rapid, safe, and prolonged local analgesic action, Pharm. Res. 29 (1) (2012) 170–177 https://doi.org/10.1007/s11095-011-0524-4.
[9] R. Hoyle, Manufacturing components for a micro litre drug delivery system, Eur Med Device Technol 1 (4) (2010).
[10] S.-E. Kim, E.C. Harker, A.C. De Leon, R.C. Advincula, J.K. Pokorski, Coextruded, aligned, and gradient-modified poly(ε-caprolactone) fibers as platforms for neural growth, Biomacromolecules 16 (3) (2015) 860–867 https://doi.org/10.1021/bm501767x.
[11] A.M. Jordan, S.-E. Kim, K. Van de Voorde, J.K. Pokorski, L.T.J. Korley, In situ fabrication of fiber reinforced three-dimensional hydrogel tissue engineering scaffolds, ACS Biomater. Sci. Eng. 3 (8) (2017) 1869–1879 https://doi.org/10.1021/acsbiomaterials.7b00229.
[12] L. Eith, R.F.T. Stepto, I. Tomka, F. Wittwer, The injection-moulded capsule, Drug Dev. Ind. Pharm. 12 (11–13) (1986) 2113–2126 https://doi.org/10.3109/03639048609042626.
[13] J.-S. Deng, M. Meisters, L. Li, J. Setesak, L. Claycomb, Y. Tian, D. Stephens, M. Widman, The development of an injection-molding process for a polyanhydride implant containing gentamicin sulfate, PDA J. Pharm. Sci. Technol. 56 (2) (2002) 65–77.
[14] M. Heckele, W.K. Schomburg, Review on micro molding of thermoplastic polymers,

J. Micromech. Microeng. 14 (3) (2003) R1–R14 https://doi.org/10.1088/0960-1317/14/3/R01.
[15] L. Eith, R.F.T. Stepto, I. Tomka, Injection-moulded drug-delivery systems, Manuf. Chem. 58 (1) (1987) 21–25.
[16] C. König, K. Ruffieux, E. Wintermantel, J. Blaser, Autosterilization of biodegradable implants by injection molding process, J. Biomed. Mater. Res. 38 (1997) 115–119 https://doi.org/10.1002/(SICI)1097-4636(199722)38:23.3.CO;2-0.
[17] M. M Crowley, F. Zhang, M. A Repka, S. Thumma, S. B Upadhye, S.K. Battu, J. W McGinity, C. Martin, Pharmaceutical applications of hot-melt extrusion, Part I 33 (2007), https://doi.org/10.1080/03639040701498759.
[18] M. A Repka, S. Majumdar, S.K. Battu, R. Srirangam, S. B Upadhye, Application of hot-melt extrusion for, Drug Deliv. 5 (2009), https://doi.org/10.1517/17425240802583421.
[19] P. Lee, J. Towslee, J. Maia, J. Pokorski, PEGylation to improve protein stability during melt processing, Macromol. Biosci. 15 (10) (2015) 1332–1337 https://doi.org/10.1002/mabi.201500143.
[20] C.D. Ryder, Method of forming and injecting thermoplastic materials, (1942) US2287277A, June 23.
[21] D.E. Dimla, M. Camilotto, F. Miani, Design and optimisation of conformal cooling channels in injection moulding tools, J. Mater. Process. Technol. 164–165 (2005) 1294–1300 https://doi.org/10.1016/j.jmatprotec.2005.02.162.
[22] A.G. Banerjee, X. Li, G. Fowler, S.K. Gupta, Incorporating manufacturability considerations during design of injection molded multi-material objects, Res. Eng. Des. 17 (4) (2007) 207–231 https://doi.org/10.1007/s00163-007-0027-9.
[23] L. Zema, G. Loreti, E. Macchi, A. Foppoli, A. Maroni, A. Gazzaniga, Injection-molded capsular device for oral pulsatile release: development of a novel mold, J. Pharm. Sci. 102 (2) (2013) 489–499 https://doi.org/10.1002/jps.23371.
[24] P.W. Lee, S. Shukla, J.D. Wallat, C. Danda, N.F. Steinmetz, J. Maia, J.K. Pokorski, Biodegradable viral nanoparticle/polymer implants prepared via melt-processing, ACS Nano 11 (9) (2017) 8777–8789 https://doi.org/10.1021/acsnano.7b02786.
[25] P.W. Lee, J. Maia, J.K. Pokorski, Milling solid proteins to enhance activity after melt-encapsulation, Int. J. Pharm. 533 (1) (2017) 254–265 https://doi.org/10.1016/j.ijpharm.2017.09.044.
[26] S.C. Clarizio, R.A. Tatara, Tensile strength, elongation, hardness, and tensile and flexural moduli of PLA filled with glycerol-plasticized DDGS, J. Polym. Environ. 20 (3) (2012) 638–646 https://doi.org/10.1007/s10924-012-0452-3.
[27] S.T. Lee, L. Kareko, J. Jun, Study of thermoplastic PLA foam extrusion, J. Cell. Plast. 44 (4) (2008) 293–305 https://doi.org/10.1177/0021955X08088859.
[28] J. Snijder, I.L. Ivanovska, M. Baclayon, W.H. Roos, G.J.L. Wuite, Probing the impact of loading rate on the mechanical properties of viral nanoparticles, Micron 43 (12) (2012) 1343–1350 https://doi.org/10.1016/j.micron.2012.04.011.
[29] Q. Guo, Thermoplastics viscosity measurement combining experimental and COMSOL simulation results, SPE Antec (2017) 270–274.
[30] R.W. Warfield, Compressibility of bulk polymers, Polym. Eng. Sci. 6 (2) (1966) 176–180 https://doi.org/10.1002/pen.760060216.
[31] S.C. Lee, D.Y. Yang, J. Ko, J.R. Youn, Effect of compressibility on flow field and fiber orientation during the filling stage of injection molding, J. Mater. Process. Technol. 70 (1) (1997) 83–92 https://doi.org/10.1016/S0924-0136(97)00041-1.